Human factors in seismic uncertainty — Restoring a realistic uncertainty range

Liz Chellingsworth[1], Mark Bentley[1], and Tim Wynn[1]

Abstract

Seismic data play a prominent part in the quantification of the subsurface. Improved imaging and calibration give us a better starting point for interpretation and uncertainty analysis. However, aside from the technical aspects of evaluating seismic data, there are human factors that play a role in the way we use and analyze the data, and these tend to work against attempts to quantify realistic uncertainty ranges. We used a case study to reveal some common pitfalls and assumptions that can compromise our ability to produce sufficiently wide uncertainty ranges in our evaluations. The example highlighted three human factors that affected the decision-making process: anchoring, availability, and overconfidence. Interpreters should avoid anchoring on a base case and focus on alternative possibilities. They should be wary of judging which methodology is best only by the ease with which it comes to mind. Technical specialists should guard against overconfidence in their data, interpretation, and ability to describe the full uncertainty space. We suggested alternative methods that allow us to restore that uncertainty range using a multideterministic approach incorporating multiple data sets, interpretations, and methodologies.

Introduction

Seismic data play a key role in the description and quantification of the subsurface in terms of structure and formation properties. Moreover, we use seismic data and seismic interpretation to help us assess uncertainty ranges and address risk in real-life field development problems. For instance, conformance of a direct hydrocarbon indicator to structure may help to delineate a prospect and reduce the uncertainty range on its lateral extents. In this case, the seismic data provide a more compelling case for the presence of an accumulation compared with a lead or prospect with no characteristic amplitude signature.

With improved imaging and calibration of our seismic data, our starting point for analysis and interpretation is enhanced, so this should help to reduce the uncertainty in the subsurface. However, aside from the technical aspects of evaluating seismic data and calibration to wells, there are human factors that play a role in the way seismic data are used, analyzed, and interpreted, and these tend to work against attempts to quantify realistic uncertainty ranges.

Research in the field of social sciences has shown that humans are overconfident in their ability to predict uncertainty (Tversky and Kahneman, 1973; Kahneman, 2011). Baddeley et al. (2004) study the underlying causes of error in information derived from probabilistic assessments made by people. Examples of how human factors can influence oil field volumetric estimates are presented by Bentley and Smith (2008) and Chellingsworth et al. (2011).

We present a case study of a seismic and mapping evaluation, in which we highlight three common heuristics that can lead to pitfalls in the assessment of uncertainty in seismic interpretation and analysis: anchoring, availability, and overconfidence. We describe ways in which we can guard against these potential problems and restore reasonable uncertainty ranges.

In many subsurface problems, uncertainty ranges tend to be narrow, centered about an initial best guess, the anchor. In the geophysics world, a simple example would be the total depth uncertainty estimation, which is typically an estimate $\pm x\%$ around a top structure depth map. The anchor (input horizon) is a nonunique interpretation of the data. The basis for the value x is often biased by a limited or skewed well data set, e.g., where wells are preferentially drilled on the crest of structures.

Another common heuristic, availability, involves adoption of a single methodology because it is the first one that comes to mind or it is the one most recently used. The danger here is that a method is adopted that is not adequate or suitable for the problem in hand. Perhaps the data set is too small or the issues in the current case are different from those in the "available" reference case.

[1]AGR TRACS, Aberdeen, UK. E-mail: liz.chellingsworth@agr.com; mark.bentley@agr.com; tim.wynn@agr.com.

Manuscript received by the Editor 12 September 2014; revised manuscript received 16 November 2014; published online 19 March 2015. This paper appears in *Interpretation*, Vol. 3, No. 2 (May 2015); p. SQ21–SQ32, 14 FIGS.

http://dx.doi.org/10.1190/INT-2014-0203.1.

Overconfidence is just that: overconfidence in our data and in our abilities to characterize the subsurface. The more experienced the practitioner, the greater the tendency toward overconfidence.

These heuristics usually emerge before the technical interpretation on a workstation begins. If the project kick-off starts with an aim to make a base or reference case interpretation on a new seismic volume (e.g., from prestack depth migration [PSDM]) with a view to reducing well-tie errors, then an anchor is already being emplaced (the base case). The work assumes the preferential use of this particular volume because it is available and there will tend to be an a priori assumption that the new volume is an improvement on the old — the seeds of overconfidence.

An alternative methodology would be to avoid — consciously — a base case, query what the limited (statistically insignificant) well data set says about the likely seismic response and start to query what is missing in the understanding of the rock properties. This line of enquiry introduces uncertainty-based logic early in the process. What sets this approach apart from the first is that we are already preparing ourselves for the uncertainty that lies ahead, accepting that we are unlikely to find the answer or solve the problem, something that many of us find uncomfortable (Bond et al., 2011).

Multideterministic approaches involve generating a small number of concepts, each of which is sufficiently different from the other to capture a wide range of possible outcomes (Bentley and Smith, 2008; Ringrose and Bentley, 2015). A base-case-led solution is likely to be misleading, whereas the multideterministic method, when carried out correctly, is more likely to prompt a workflow that uses a range of methodologies to evaluate a broad uncertainty space.

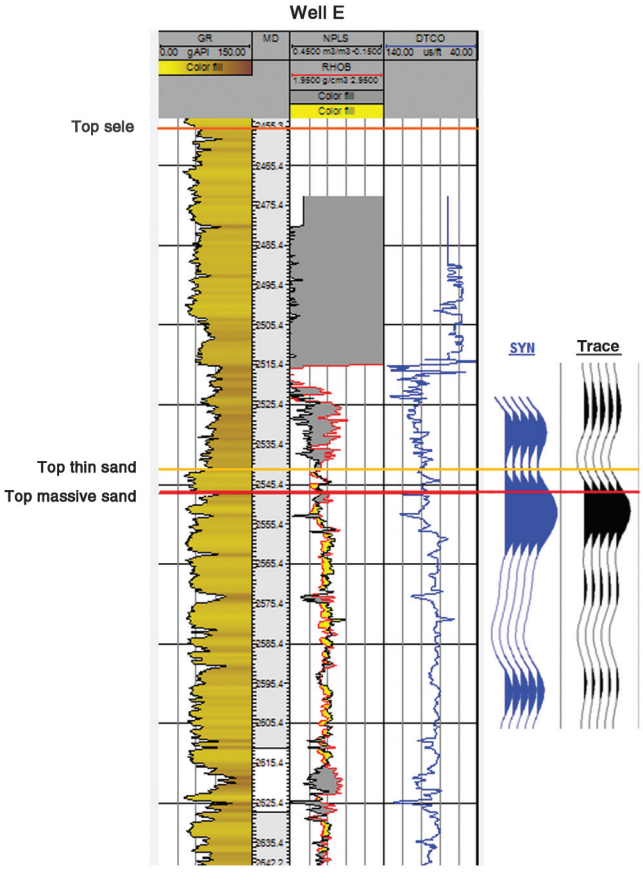

Figure 1. Well E is located at the crest of the field. The reservoir consists of a thin upper sand overlying well-developed massive sand.

Method

Introduction

We present a case study to demonstrate some common heuristics and suggest alternative approaches to avoid the pitfalls of those behaviors. Our case study focuses on the Nefertiti field, an oil field located in the UK sector of the North Sea. It is a Paleocene oil accumulation characterized by well-developed turbidite sands (Figure 1, discovery well, well E) within a relatively low relief, compaction structure (Figure 2). The field can be divided into two areas. The main part of the field captures the main structural high with the discovery well (well E) at the crest (Figure 2). The north part is characterized by a much lower relief structure, which is more poorly defined on seismic data and has not been penetrated by any wells. Note that all field and well names have been changed to maintain anonymity, and axes have been removed from maps.

The field has been developed by two horizontal producers, both located in the Main field. Well N01 was drilled across the axis of the fairway with the production

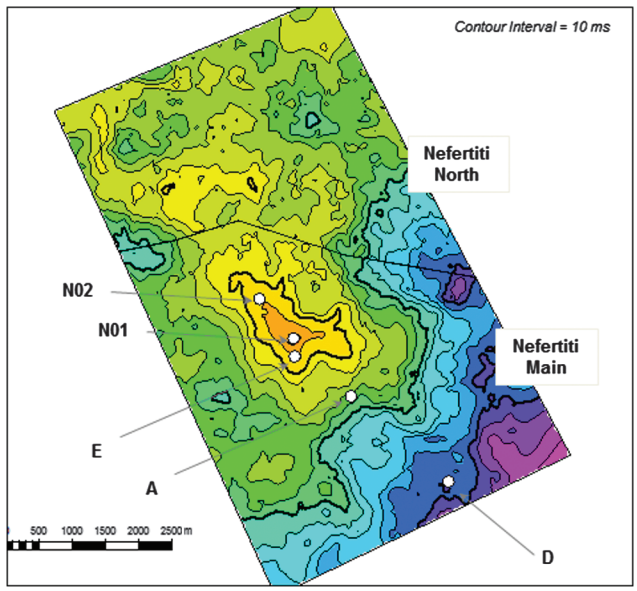

Figure 2. Time structure map in ms two-way traveltime (TWT) based on one of the 2013 horizon interpretations. The exploration and appraisal wells (E, A, and D) are shown, and the two producers (N01 and N02) are highlighted. Nefertiti North is a low-relief structure north of the producing area.

performance indicating the edge water drive; i.e., oil is driven through the reservoir by aquifer water moving in from the edges. Well N02 was drilled along the axis, and production is more characteristic of bottom drive; i.e., water is moving in from the aquifer below. The aim of the study was to assess remaining opportunities within the main field and to identify whether there is a viable target in the north, in terms of in-place and recoverable resources.

The objectives of the geophysical review were to generate a range of top structure depth maps to assess structural uncertainty of the developed Nefertiti Main area and the undrilled Nefertiti North area. The resulting maps were used in the reservoir modeling process to derive a range of stock tank oil initially in place (STOIIP) estimates, which in turn formed the basis of the dynamic analysis, ultimately leading to a range of remaining oil-in-place maps.

The costs of drilling, completing, and tying back wells are high, and the company had recently suffered a poor well result in a similar geologic and geophysical setting. It was, therefore, important to ensure that the full uncertainty range was addressed prior to making another investment decision.

The last evaluation of the field dated back to 2010 when the operator reprocessed the seismic data and generated various reflectivity, colored inversion, and elastic inversion cubes across Nefertiti and the wider area. The resulting data volumes were of high quality with a marked improvement in the signal-to-noise ratio (S/N). Rock-physics analysis indicated that seismic attributes could be used to discriminate between fluid and lithology, in areas where massive sands are present; however, where sands are thin or thinly bedded, seismic attributes are unreliable.

At that time, the operator focused the uncertainty analysis on (1) the mapping of the top structure from the various data sets and (2) a depth conversion using new PSDM velocities. After a second phase of reprocessing in 2013, the interpretation was revisited and the uncertainty analysis was expanded. Remaining uncertainties surrounding the top structure depth were identified and investigated.

Horizon interpretation

Historically, horizon interpretations over the field result in high-rugosity structure maps (Figure 2). The magnitude and locations of the small-scale "lumps and bumps" vary considerably depending on the interpreter and the input seismic data, e.g., full stacks versus partial stacks and reflectivity versus inversion volumes (Figure 3). The variability increases away from the core area to the fringes, i.e., from the location where the sands are thick to where they are less well developed. The north also shows a high degree of variability depending on the volume used. These points are illustrated in Figure 4,

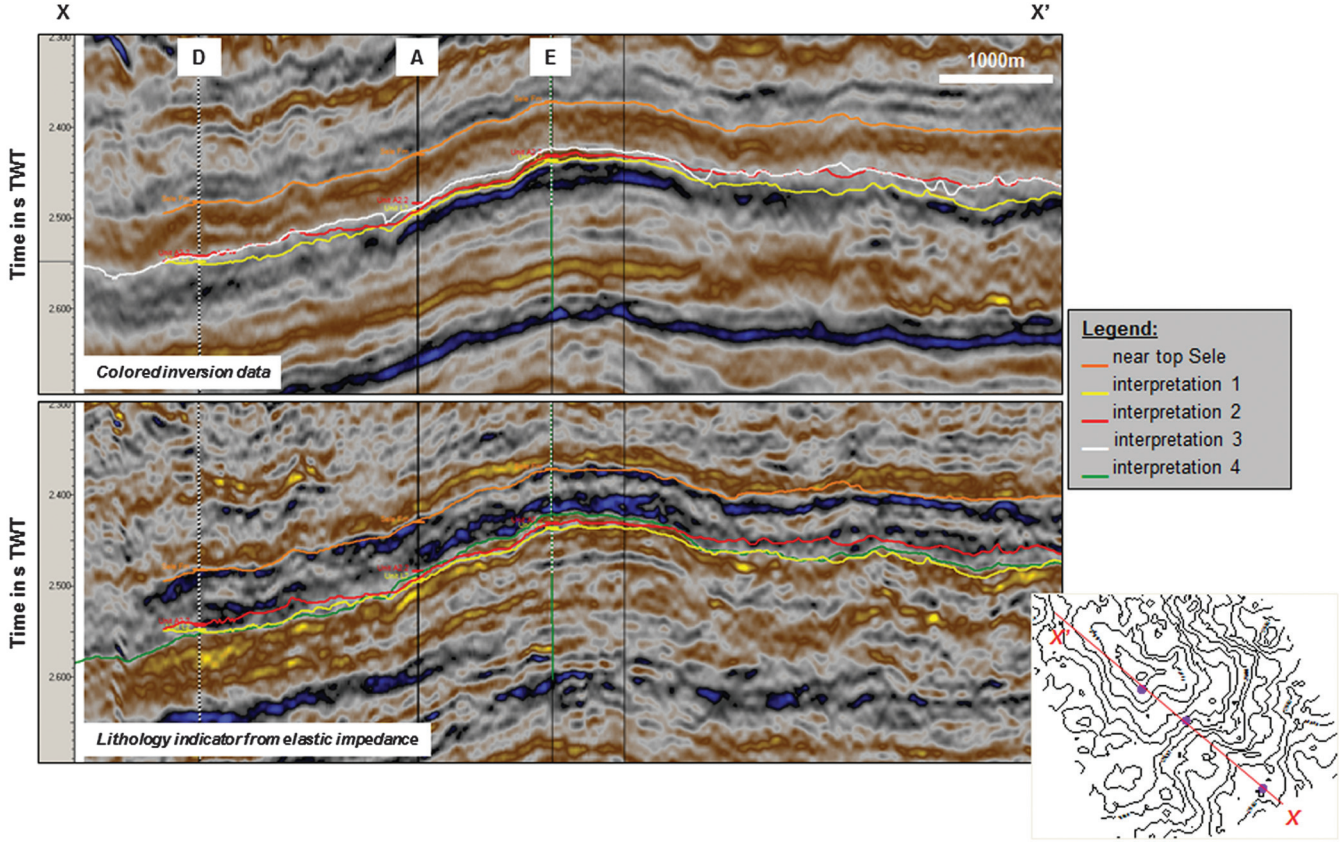

Figure 3. A well-tie line taken from two different seismic data sets highlights the similarities and differences in reservoir expression. Four horizon interpretations are indicated.

which shows a difference map of two of the horizon interpretations.

The question arises as to which seismic data set is the best input for a mapping workflow. If the seismic processing is robust for all seismic volumes, there is no direct answer to this question — all are plausible inputs generating slightly different outputs.

In fact, the rugosity and variability observed here are not atypical of Paleocene turbidite fields elsewhere in the North Sea. Examples from fields in UK continental shelf quadrants 15 and 16 (approximately 225 km [140 mi] to the northeast of Aberdeen) show that with each acquisition and round of seismic processing and new interpreter, the lumps and bumps on the structure maps move around and even disappear altogether. This effect is sometimes referred to as the "cat under the carpet," and it is the reason why many small prospects remain undrilled (or drilled with disappointment). Understanding the possible variations in the shape of a reservoir is important because it can have an impact on production performance and it influences decisions during well planning or development planning (Piquet et al., 2013).

One way of capturing the variability in horizon interpretation would be to use a stochastic approach. A horizon is interpreted from the best-quality seismic data set, where the term "best-quality" can refer to the highest S/N or the most robust data type. The variability of the picked horizon is modified using an algorithm that adds or subtracts lumps and bumps to the input horizon according to certain rules describing parameters, such as the following:

- number, shape, size, and magnitude
- maximum allowable gradient and change in gradient

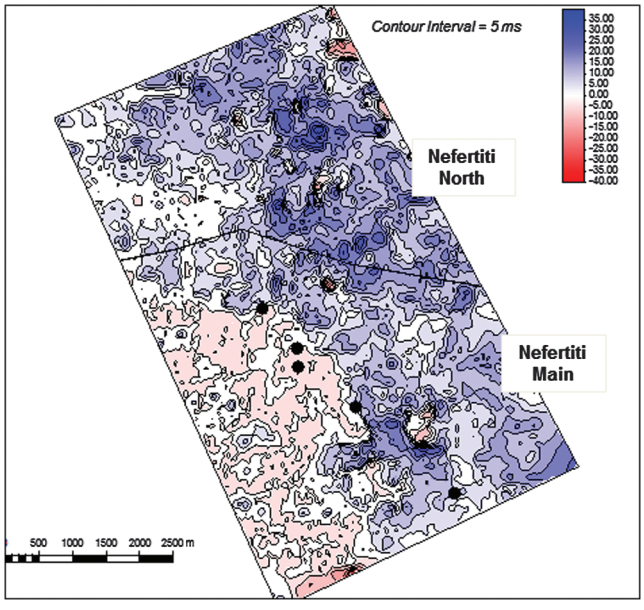

Figure 4. A difference map between two horizon interpretations illustrates the variability in interpretation away from the core area.

- connectivity, i.e., how much features can join up to form ridges or troughs.

Ranges are defined for each parameter, and the algorithm randomly selects from each of those parameters to produce a very large number of maps with varying degrees of rugosity. Although the above method represents a feasible and mildly interesting coding project, none of the output maps can be related to an actual interpretation or input data set, which can cause problems down the line, e.g., during well planning.

Furthermore, they are all based on the original input horizon (the anchor) and are, therefore, statistically center weighted to an interpretation that is not likely to be a P50. Invariably, any preferred case that is derived from the stochastic realizations would tend to deliver the initial anchor. The workflow would have explored the defined range, but it would return a "best estimate" that reflects the initial interpretation, thereby negating the whole purpose of the exercise.

Instead of anchoring on a single interpretation, it is useful to capture the variability in horizon interpretation by including a discrete number of distinctly different horizons, each based on a different input data set. For instance, in one map, the north might consist of two to three very flat structures with no defining closing contour, whereas on another map, the north might form a more prominent feature with some degree of structural closure.

The multideterministic approach, i.e., incorporating distinct and alternative interpretations, has the advantage that each map is linked to a real-time interpretation, to something that the interpreter saw on the data and processed in his or her brain. In addition, there is no reliance on a single seismic cube or data type. Horizons picked on reflectivity can be analyzed alongside those picked on impedance data, recognizing that both data sets have advantages and disadvantages.

In this case, we use three seismic data sets from the 2013 suite of cubes (all prestack time migration [PSTM]) to generate a top structure time horizon: a colored inversion cube, a (full offset) reflectivity cube, and a lithology indicator from elastic impedance. One of the horizon interpretations was discarded because it showed a very high degree of similarity to one of the others; effectively, it is a duplicate. In addition, we include two horizon interpretations from the 2010 evaluation. The resulting four inputs form the basis of the next step in the mapping uncertainty analysis.

Depth conversion — Introduction

The 3D seismic survey covers an area of approximately 150 km^2 and comprises three producing fields. Nefertiti itself makes up less than 25% of the survey area. In total, there are 11 wells located within the survey area: 9 wells are spread across three producing fields and the remaining 2 wells are located between fields. Not all wells have a sonic log, and there are limited check-shot/vertical-seismic-profile data available;

the time depth data set is thus incomplete. Seismic velocity data were available and were used extensively by the operator in previous evaluations. All available well data were incorporated in the current analysis and in the derivation of averages, functions, maps, and trends. Note that the interpreted horizons themselves are limited to the Nefertiti field.

The 2010 depth conversion analysis was based on the PSDM velocities that cover Nefertiti and the wider area. The velocity cube incorporates corrections for high-velocity injected sands of Eocene age that are known to occur throughout the basin and that can give rise to velocity pull-ups at reservoir level, a problem evaluated by Rowbotham et al. (2010).

Injected sands are seen in the wells throughout the license block, and some of the larger features are imaged on seismic data (Figure 5); however, numerous smaller injectites observed on logs are not imaged at all. Sometimes, the fast sands occur in clusters; in other places, they appear to be isolated. Furthermore, their interval velocity and thickness vary quite markedly between wells and even within wells.

There is clearly uncertainty in the distribution and effect of the fast sands on the position of the top reservoir reflection. There are also limitations to the lateral and vertical resolution of the seismic data and velocity cubes. The 2010 velocity cube represents a single, possible solution for the correction for the Eocene sands. It would actually be very difficult to prove that it provides a complete solution for all injected sands.

PSDM velocity cubes are created for optimal imaging, not exact depthing. Alternative velocity cubes could be generated to derive a range of plausible solutions to the injected sands problems, e.g., using different assumptions about size, distribution, and velocity of the injected sands. The underlying assumption, however, is that we are able to make reliable predictions about all of these parameters and capture or accommodate them adequately in the velocity cube. We are being overconfident in our ability to estimate what the subsurface looks like.

Various depth conversion methods exist that allow for more, less, or even no correction for the fast sands. Although some of these methods are basic or require less effort in terms of processing, they do allow fundamentally different approaches and assumptions to be included in the analysis, and some of these methods are considered below. More advanced methodologies, e.g., full-waveform inversion , typically require a greater time and cost investment, but they could be included at a later stage if the initial screening results proved to be promising.

Depth conversion — Methods

We investigate a range of depth conversion techniques without singling out a particular method prior to selecting representative low, mid, and high case maps. Again, we are trying to avoid anchoring on a single method.

Method 1: V_{cube}

The operator provided an updated PSDM velocity cube, which incorporates corrections for the fast sands. We generate a velocity model and process the various input horizons. The resulting depth surfaces effectively represent an update to the 2010 method.

Method 2: V_{avg}

The values of average velocity (V_{avg}) calculated from the surface to the top reservoir are analyzed for all the wells in the area of interest, and a mean value is calculated. It is a crude method, but it forms a useful starting point for quality-control checks on the well data set

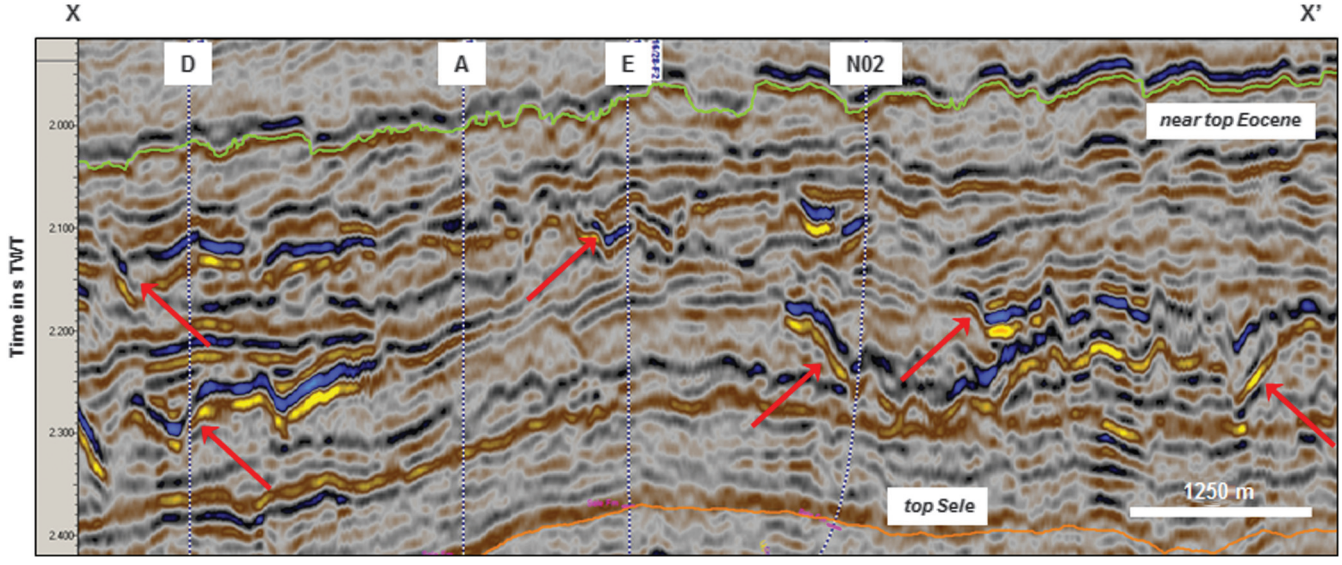

Figure 5. V-shaped features, often associated with high amplitudes, are present in the Eocene interval and correspond to large injectites. Numerous wells in the area have penetrated injected sands; the larger ones can be tied to the seismic data.

themselves and can provide some insights into issues such as large fluctuations between adjacent wells and geologic trends.

Method 3: V_{map}

In the V_{map} workflow, the V_{avg} points are interpolated using a convergent interpolation algorithm to form a velocity map over the entire license block (Figure 6). This allows some of the time depth variations related to basin shape and overburden thickness to be captured. Here, we see a steady increase from northwest to southeast, which is consistent with the basin shape and previous experience in the wider area. It is clear that this method is not a substitute for a "layer-cake" depth conversion, but it does start to capture some of the lateral geologic trends. Other interpolation algorithms were tested, but none captured the strong basin trend observed in the data.

Method 4: V_{lin}

We test various linear functions from time-depth pairs in the wells. Some functions use all the wells in the area; others include only the Nefertiti wells. Most wells plotted close to a straight line with only the downdip D well lying off trend.

Method 5: V_{trend}

The fast Eocene sands (injectites) were considered to be a particular issue, so it became desirable to evaluate other methods that could overcome any pull-up effects that we suspect are embedded in the data. The operator had previously carried out a regional study covering a much larger area to investigate methods of correcting for the fast sands. The operator developed a technique that involved applying a regional correction map to the top reservoir horizon in time prior to depth conversion. The sum of negative amplitudes (SNA) over the fast sands at the wells is crossplotted against the thickness of those sands. A function is fitted through the data points and applied to the SNA map to generate a regional correction map, which is then added to the time map prior to depth conversion.

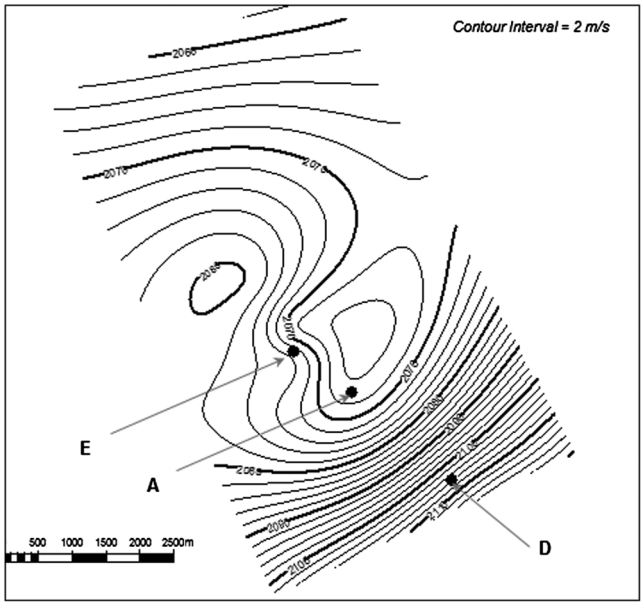

Figure 6. The average velocity map (surface to top structure) is based on data from the entire license block. The map shows a general increase in V_{avg} from the northwest to the southeast.

The regional correction function was developed on the basis of a large number of wells, and it has proved to be successful in improving depth prediction away from wells at a large scale, i.e., in regional studies. For more rigorous depth conversion over single fields, however, such a semiquantitative approach may not be appropriate for several reasons. First, on closer inspection of the Eocene sands, it is clear that the sonic profile within a fast sand is not uniform and can vary considerably, such as in well V (Figure 7). Bear in mind that the sonic profile can be hugely influenced by near-borehole effects and textural features in injected sands. Second, seismic amplitudes are affected by numerous parameters including thickness, fluid fill, tuning, acquisition artifacts, etc. Any amplitude map used as a fast-sands indicator will inevitably capture effects that are not related to high-velocity Eocene sands. Finally, detailed analysis from the current study has indicated that correction functions and resulting correlation coefficients are highly dependent on the following:

- which wells are included/excluded in the data set
- how sand thickness is selected: entire box car sand or only the fastest part
- type of amplitude extraction: SNA versus root-mean-square
- software used for amplitude extraction
- window of amplitude extraction.

We revisit the analysis using only the wells (or a subset of the wells) in our area of interest. We test several "local" functions using combinations of the variables above to investigate the possibility of generating a robust "local" correction map. Figure 8 shows one example of a local correction function. In general, the correlation coefficients tend to be low, at best 0.7 and down to <0.5. Also, the resulting correction maps were quite different. We spot checked correction values and in some places the correction was inferred to be quite large (>40 ms). These large values were sense checked against the seismic data. In theory, such large values should manifest themselves as a discernible velocity effect; however, that was not the case.

None of this analysis invalidates the regional work; it merely suggests that the regional solution is not appropriate for the current problem. We suggest that a semiquantitative approach may be misleading and could generate false confidence in the results. Therefore, a "softer" V_{trend} approach was adopted, whereby the SNA map is applied as a trend map to the average velocity map to make local velocity corrections (Figure 9). We

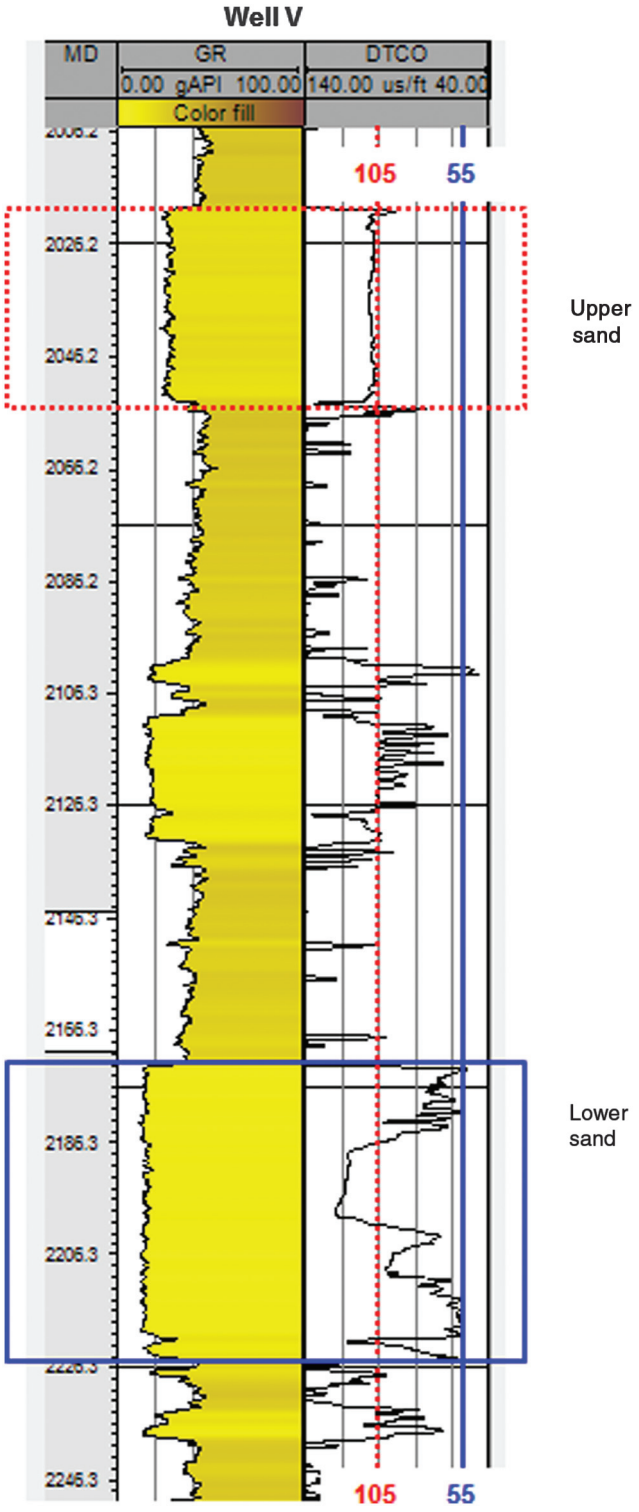

Figure 7. Well V further north in the license block penetrated several large injectites. The sonic profiles vary considerably between the upper and lower sands and even within the lower sand. The upper sand has a sonic value of 105 μs/ft (red stippled line). The lower sand has a boxcar signature on the gamma ray, but clearly the sonic value varies quite dramatically from ~55 to ~120 μs/ft and back to 55 μs/ft (blue solid line).

thus recognize that the method can help to honor gross trends without forcing the regional solution onto a local problem.

Well-tie radius

A lot of time and focus was put on the horizon interpretation and depth conversion, but previous studies had also flagged that the well-tie method and radius R influence resulting depth maps significantly. Although not strictly a geophysical issue, the well-tie method and radius can in some cases have a much greater impact on depth uncertainty than other factors. This is especially true for fields that are relatively flat, where well ties are difficult and the overburden is complex.

In this case study, we consider a simple well-tie method, namely, using a fixed radius around the wells to flex the depth map to the correct position in depth at the wells. This is a technique that works relatively well for minor residual errors and fields that are small. In instances in which there are numerous wells available, other techniques may be more appropriate, such as neural networks or geostatistical methods (Bartel et al., 2006).

Disappointingly, the selected well-tie radius is often the default parameter in the software package of choice. Ideally, we should consider parameters such as magnitude of errors at the wells, well spacing, gradient, and structural/depositional trends during the selection process. Previous experience of similar fields in the area (size and relief) indicates that a well-tie radius between 400 and 2500 m is appropriate, depending on the magnitude of the residual errors and the size of the field.

It is useful to step back and contemplate the lateral extents of the perturbation associated with residual corrections for a range of well-tie radii (Figure 10). The example shows the theoretical residual maps for a uni-

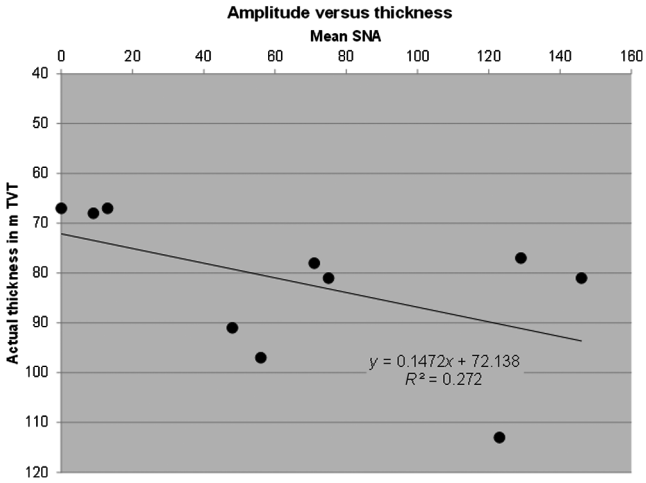

Figure 8. A sample plot from wells in the area with average SNA plotted against actual (injectite) sand thickness in the wells. The regression line through the points has a poor correlation coefficient.

form error of 20 m at the wells and a variable radius of influence. The outer areas are not affected (zero correction); at the wells, the maximum correction applies.

For a small radius, $R = 400$ m, the perturbation is localized, as expected. For a large radius, $R = 1500$ m or greater, the whole of the core area is modified and the southern part of Nefertiti North is also affected. For a broad, flat structure, the impact on the gross rock volume (GRV) will be significant. Area-depth charts provide a powerful way of visualizing the impact of the well-tie radius. In our case study, Nefertiti North disappeared completely at a certain well-tie radius, regardless of the input horizon or depth conversion method.

For sensitivity, we test a two-stage well-tie correction. This involved tying the surface to the picks in the vertical wells only — prior to applying a well tie to the tops in the horizontal wells. By tying the wells in two stages, the gross residual error is corrected and only a minor adjustment is needed at the horizontal wells. The radius of influence still has an impact in the first stage, but less so during the second stage. This may reflect some of the inherent uncertainty in deviation surveys of horizontal wells. Finally, we also test the impact of applying some form of mean bias to the raw depth surfaces before correcting to the wells. Three types of mean bias were investigated, but their effect was similar to that of going from a well tie with $R = 1500$ to one with $R = 2500$.

The analysis demonstrates that the well-tie radius has a significant impact on GRV. To address adequately the uncertainty in the well-tie radius, a single "anchored" or software-default radius was rejected and a range of values considered instead.

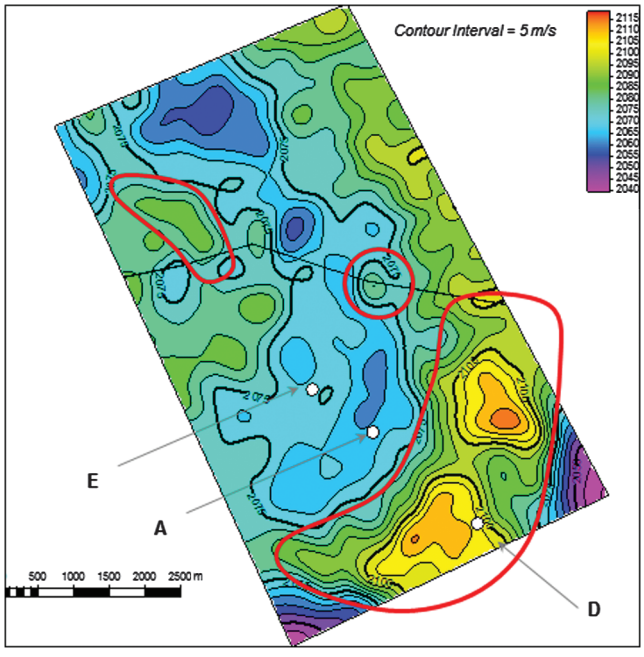

Figure 9. The V_{trend} map incorporates a qualitative trend from the SNA analysis to try and account for the effect of the fast sands. The location of these injectites is shown in red outline.

Results

Results show that the size, shape, and volume of the Nefertiti Main and Nefertiti North are very sensitive to the selected input horizon, depth conversion, and well-tie radius. We quantify these observations using the parameter GRV (above contact). The aim of the exercise was to aid selection of low, mid, and high maps for input into the static model. Implicit in our analysis is that the contact in the north is the same as in the main field. Clearly, without a well in the north, this is an assumption: one that may be incorrect. The study could be expanded to include alternative contacts.

We calculate and tabulate the GRV for multiple (logical) combinations of input horizon, depth conversion, and well-tie radius. This allowed us to assess the uncertainty range and evaluate the impact of any single parameter. To quantify or benchmark the effect, we select a comparison case, the horizon that most closely mimicked the operator's previous final depth map, to allow comparison with other GRV estimates. Note that the comparison case is used only to quantify variations in the tornado plots — It was not selected as "the reference case."

In the first pass, the input horizon and radius of influence ($R = 1500$ m) were locked and we varied the depth-conversion method (Figure 11). The V_{cube} method was consistently optimistic, but the other methods produced broadly similar results. It is clear that a suite of low, mid, and high maps based solely on maps using the V_{cube} method would be anchored around an optimistic case yielding a skewed uncertainty range.

Next, the input horizon and depth conversion method were kept the same, but we vary the radius of influence from $R = 400$ m (local) to $R = \infty$ (aka global). When using an infinitely large radius, the Nefertiti structure shrinks to a small core area and Nefertiti North disappears below the contact. As the radius is decreased, the size of the structure above the contact increases and Nefertiti North appears above the assumed oil water contact. At even smaller radii, the Nefertiti structure swells considerably and becomes connected to Nefertiti North above the contact. These are all plausible geometries for the field and its northern extension.

In total, we calculated the GRV for over 50 cases (Figure 12). In a blind test, the geologist selected three cases from the histogram of cases (low, mid, and high). We did not provide any information as to the origin of those cases. The selected maps showed a credible range of GRV variation across Nefertiti Main and Nefertiti North and were plausible combinations of the various parameters. The low case map (Figure 13) has a negligible GRV in Nefertiti North and a modest GRV in the Nefertiti Main area. The mid map has a larger GRV in the Nefertiti Main field as well as an increased GRV in the Nefertiti North field. We felt that a representative mid case should have some GRV associated with

Nefertiti North for two reasons: First, the northern structure is consistently interpreted as a (minor) structural high and appears on most depth maps generated to date. Second, for assessing the potential of a well placed in the north, some volume is required. If it is not there, we cannot evaluate it. The high case map (Figure 13) has a much larger structure in the north and a GRV that is sizeable yet compatible with dynamic data. The very highest end of the GRV histogram graph was not considered because these depth realizations tended not to show any signs of closure around the core area of Nefertiti and were inconsistent with indications from dynamic data.

When looking at the 18 cases that make up the very high end, it is interesting to see that there is no single input map, depth conversion, or well-tie method that consistently gives these high GRVs. The combination of the V_{cube} method with one of the 2010 maps produces the very largest GRVs. These maps account for 30% of the discarded cases; the other 70% of rejected cases are derived from a range of inputs and methodologies. This suggests that on the whole, the individual components or inputs are realistic but the total combination of some inputs generates implausible results. By analyzing the GRVs and the depth maps at this stage of the process, i.e., before progressing to the full STOIIP analysis, we are able to remove or truncate the ultrahigh (and unrealistic) part of the range.

It is noticeable from Figure 14 that the current maps are more optimistic for Nefertiti North than the previous maps (as indicated by the comparison case). There may be a simple and human reason for this: The team members who worked on Nefertiti prior to 2013

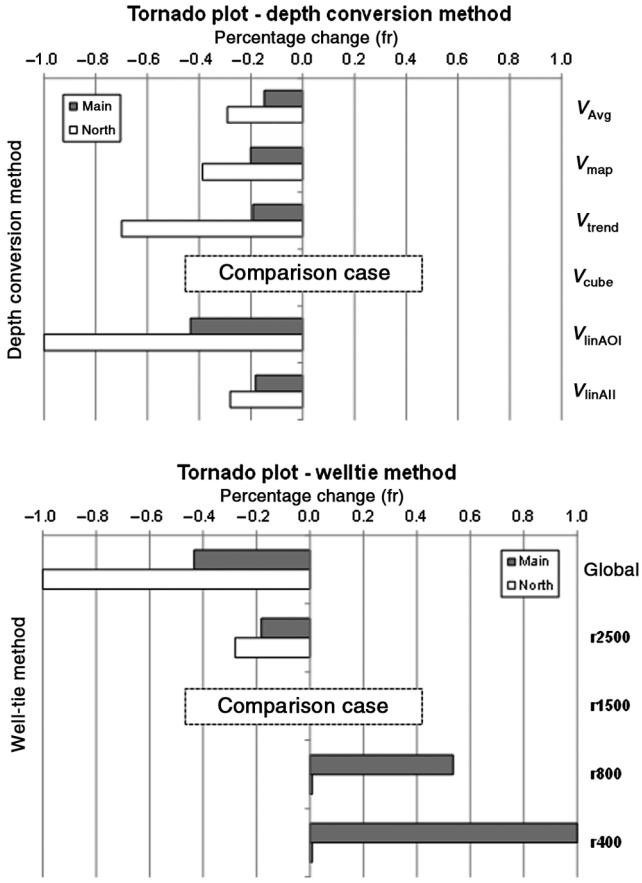

Figure 11. Two tornado plots showing the impact of the time-depth method and well-tie radius on GRV as a percentage change relative to the comparison case. The impact on GRV in Nefertiti North is remarkable.

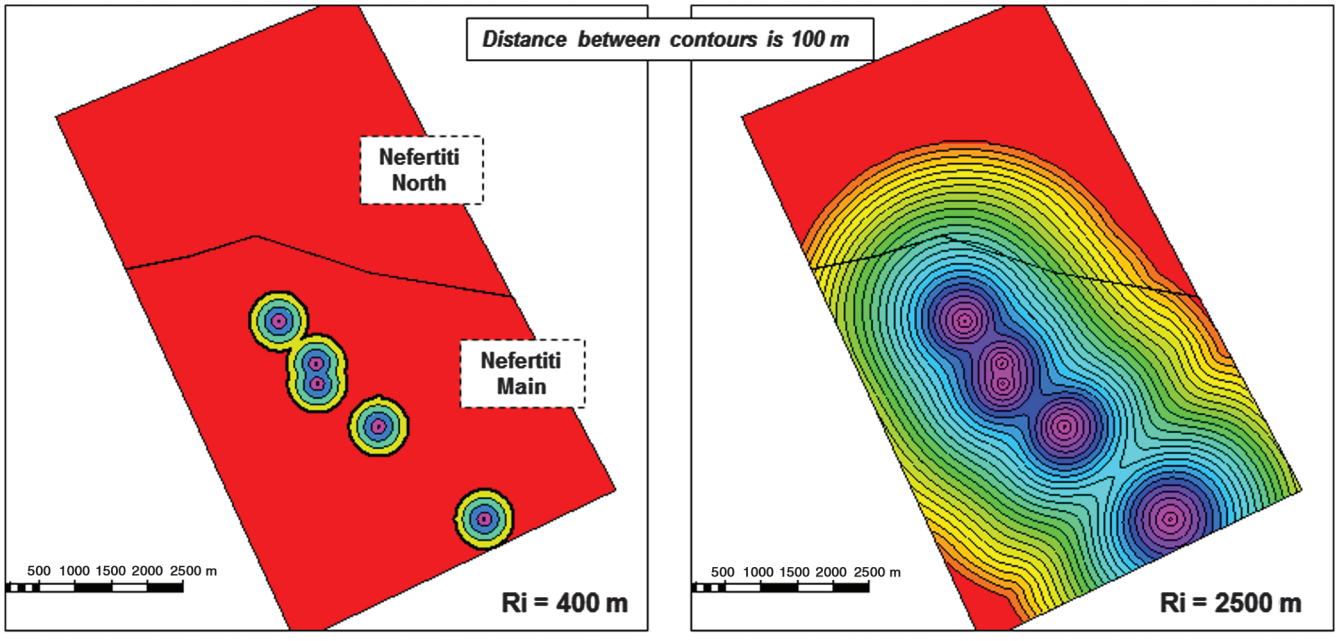

Figure 10. An illustration of the influence radius of the well-tie process. In the case of a large R, the entire core area is affected and a large part of Nefertiti North is also modified.

were also involved in the drilling of a nearby look-a-like structure, the Creon field. The results of test drilling on this structure were disappointing, with pay sands encountered deeper and thinner than expected, and the well was considered a failure. Such an experience could lead to emotional bias — "loss aversion" (Kahneman, 2011) — against any look-a-like structure, in this case, Nefertiti North. For instance, we may choose to adopt a cautious depth conversion method that "kills off" the prospect completely (GRV = zero) or radically reduces its size because we feel that the prospect is likely to be a commercial failure. The reasoning behind this is that if it is not there, we cannot drill it and thus cannot meet failure.

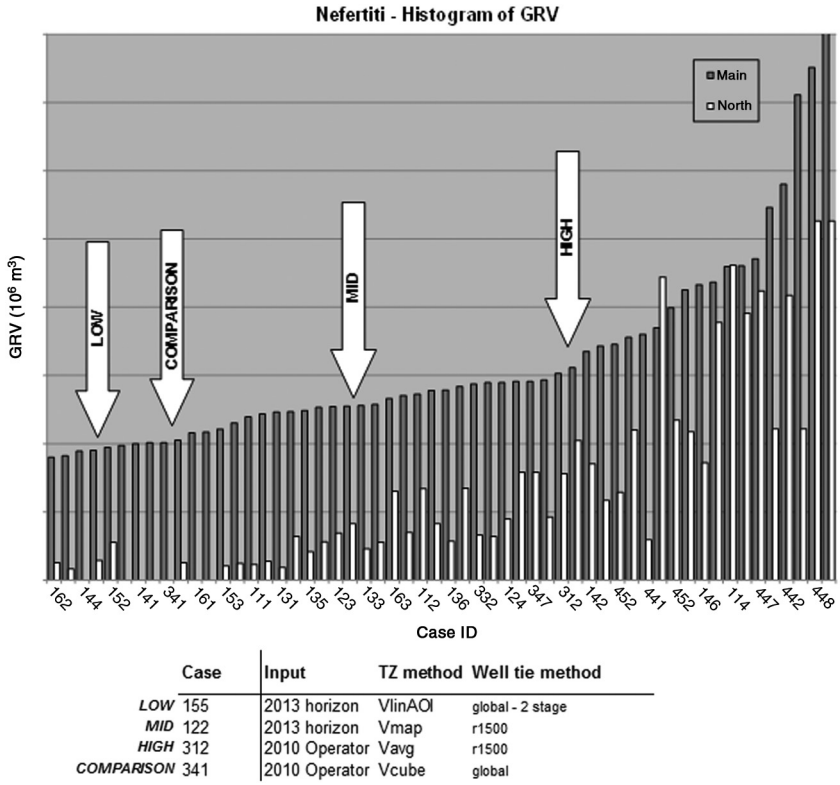

	Case	Input	TZ method	Well tie method
LOW	155	2013 horizon	VlinAOI	global - 2 stage
MID	122	2013 horizon	Vmap	r1500
HIGH	312	2010 Operator	Vavg	r1500
COMPARISON	341	2010 Operator	Vcube	global

Figure 12. Full range of cases evaluated with the final low, mid, high, and comparison cases highlighted. The table of input parameters indicates that no single horizon, depth conversion method, or well-tie radius was selected.

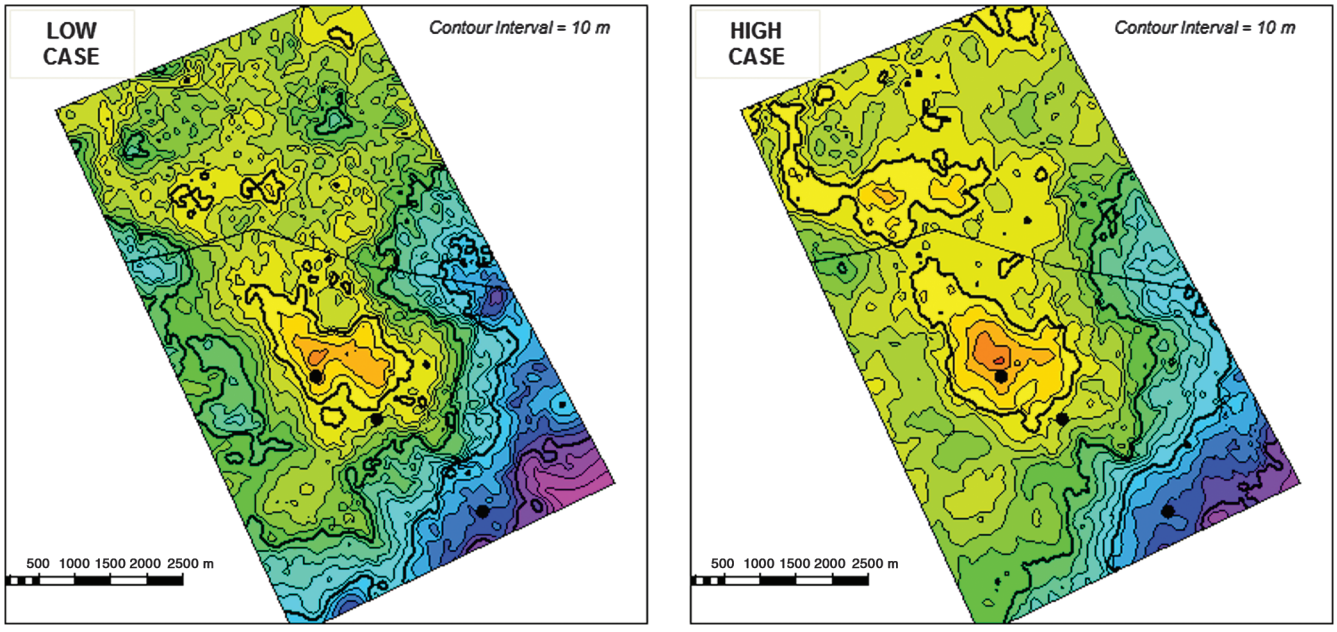

Figure 13. The selected low and high case depth maps show clear differences over the main and north parts of the field.

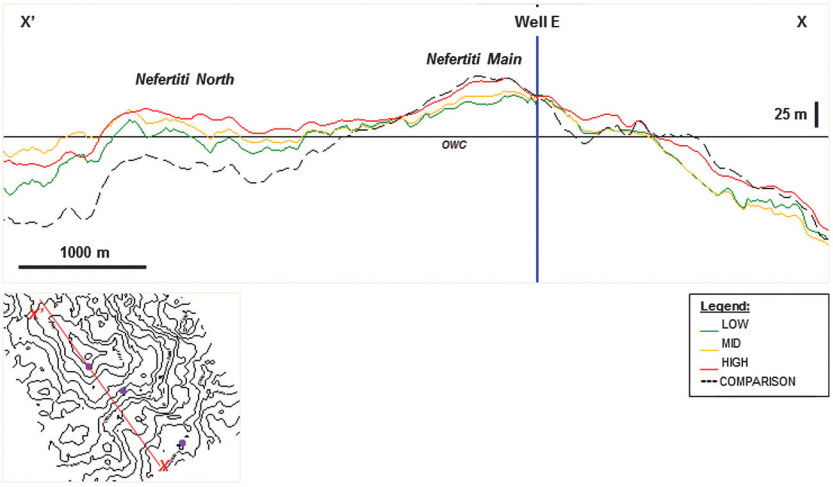

Figure 14. The selected cases plotted up alongside the comparison case show the wide variation in structure across the south part and the undrilled north. Note that the comparison case is optimistic over the main part of the field but pessimistic in the north.

Conclusion

Human factors can affect the way we estimate or evaluate uncertainty during a geophysical study. We looked at three main factors that can result in a range being too narrow: anchoring, availability, and overconfidence. During our analysis of the Nefertiti field, we took great care not to be influenced by these factors.

We evaluated the depth uncertainty of the Nefertiti field by incorporating three main areas of uncertainty: the input horizon, depth conversion method, and well-tie radius. To avoid anchoring on a single input, we generate a horizon based on three available seismic volumes, each one of high quality but emphasizing slightly different aspects. We also included additional horizons from a previous study into the analysis; they remain after all valid inputs.

We selected several depth-conversion methods ranging from very simple to more complex. The most "available" depth-conversion methods were to use the velocity model or the preexisting regional correction map, both of which try to adjust for fast sands in the Eocene. Because we cannot be confident that we can predict or characterize the fast sands accurately, we use a softer method incorporating a trend map instead of using a semiquantitative approach.

We investigated the impact of the well-tie radius on depth uncertainty and discovered that it had a significant effect on the North area. We had to take care not to be biased by previous experiences of drilling such low-relief structures.

In total, 50 combinations of parameters gave the final range of depth maps. Representative low, mid, and high cases were selected, each associated with a different set of inputs. It is clear from this method that we did not preselect inputs or methodologies to define the low, mid, and high maps.

The maps were used as inputs to the full STOIIP analysis, and the reservoir team evaluated the potential of an infill well in Nefertiti Main. In Nefertiti North, the three maps selected for use in the static modeling gave realizations with negligible, small, and modest volumes of oil allowing the reservoir team to evaluate a potential well in the north. In this area, it was the dynamic behavior, in particular, the drive mechanism (edge drive versus bottom drive), that dominated recovery potential. Again, this is a common observation in other fields in the basin.

The observations from the seismic uncertainty analysis underline the risk to closure in Nefertiti North, i.e., structural trap. However, stratigraphic trapping is extremely common in analog fields in the area and in some cases forms the main trapping mechanism. We should also be careful not to mix risk (Is there a trap?) and uncertainty (Is the trap small?) and thus "double dip" when quantifying the uncertainty range. Although Nefertiti North carries a risk to trap (and indeed reservoir presence), experience from the wider basin shows that structures of similar size that have been drilled generally do trap and contain oil.

Decision makers rely on technical people making a thorough and unbiased analysis of the data. As humans, we are prone to bias, and we are unlikely ever to mend our ways entirely. However, if we are aware of some of the pitfalls that may arise in our assessment of uncertainty in the seismic domain, we can at least begin to restore the range, instead of fearing uncertainty and chasing the elusive answer.

Acknowledgments

We would like to thank the operator for permission to publish this case study. We appreciate the contribution of all colleagues whose ideas and discussions have led to this paper.

References

Baddeley, M. C., A. Curtis, and R. Wood, 2004, An introduction to prior information derived from probabilistic judgments: Elicitation of knowledge, cognitive bias and herding: Geological Society London, Special Publications, **239**, 15–27, doi: 10.1144/GSL.SP.2004.239.01.02.

Bartel, D. C., M. Busby, J. Nealon, and J. Zaske, 2006, Time to depth conversion and uncertainty assessment using average velocity modeling: 76th Annual International Meeting, SEG, Expanded Abstracts, 2166–2170.

Bentley, M., and S. Smith, 2008, Scenario-based reservoir modeling: The need for more determinism and less anchoring: Geological Society London, Special Publications, **309**, 145–159, doi: 10.1144/SP309.11.

Bond, C. E., C. Philo, and Z. K. Shipton, 2011, When there isn't a right answer: Interpretation and reasoning, key skills for 21st century geoscience: International Journal of Science Education, **3**, 629–652, doi: 10.1080/09500691003660364.

Chellingsworth, L., M. Bentley, P. Kane, K. Milne, and P. Rowbotham, 2011, Human limitations on hydrocarbon resource estimates — Why we make mistakes in data rooms: First Break, **29**, 49–57, doi: 10.3997/1365-2397.2011013.

Kahneman, D., 2011, Thinking, fast and slow: Penguin.

Piquet, G., F. Pivot, and A. Forge, 2013, Geomodel geometry distorted by seismic velocity uncertainties: Presented at SPE Reservoir Characterization and Simulation Conference.

Ringrose, P., and M. Bentley, 2015, Reservoir model design: Springer.

Rowbotham, P., P. Kane, and M. Bentley, 2010, Bias in geophysical interpretation — The case for multiple deterministic scenarios: The Leading Edge, **29**, 590–595, doi: 10.1190/1.3422459.

Tversky, A., and D. Kahneman, 1973, Availability: A heuristic for judging frequency and probability: Cognitive Psychology, **5**, 207–232, doi: 10.1016/0010-0285(73)90033-9.

Biographies and photographs of the authors are not available.